arXiv:0711.1248v2 [hep-ph] 18 Dec 2007

DO-TH 07/08
October 2007

Dynamical NNLO parton distributions and the perturbative stability of $F_L(x, Q^2)$

M. Glück[1], C. Pisano[2], E. Reya[1]

[1] *Universität Dortmund, Institut für Physik*
D-44221 Dortmund, Germany

[2] *Vrije Universiteit, Dept. of Physics and Astronomy*
De Boelelaan 1081, NL-1081 HV Amsterdam, The Netherlands

Abstract

It is shown that the previously noted extreme perturbative NNLO/NLO instability of the longitudinal structure function $F_L(x, Q^2)$ is a mere artefact of the commonly utilized 'standard' gluon distributions. In particular it is demonstrated that using the appropriate – dynamically generated – parton distributions at NLO and NNLO, $F_L(x, Q^2)$ turns out to be perturbatively rather stable already for $Q^2 \geq \mathcal{O}(2-3$ GeV$^2)$.

A sensitive test of the reliability of perturbative QCD is provided by studying [1, 2, 3, 4] the perturbative stability of the longitudinal structure function $F_L(x,Q^2)$ in the very small Bjorken-x region, $x \lesssim 10^{-3}$, at the perturbatively relevant low values of $Q^2 \gtrsim \mathcal{O}(2-3$ GeV$^2)$. For the perturbative–order independent rather flat toy model parton distributions in [1], assumed to be relevant at $Q^2 \simeq 2$ GeV^2, it was shown that next–to–next–to–leading order (NNLO) effects are quite dramatic at $x \lesssim 10^{-3}$ (cf. Fig. 4 of [1]). To some extent such an enhancement is related to the fact, as will be discussed in more detail below, that the third–order α_s^3 contributions to the longitudinal coefficient functions behave like $xc_L^{(3)} \sim -\ln x$ at small x, as compared to the small and constant coefficient functions at LO and NLO, respectively. It was furthermore pointed out, however, that at higher values of Q^2, say $Q^2 \simeq 30$ GeV^2, where the parton distributions are expected to be steeper in the small–x region (cf. eq. (13) of [1]), the NNLO effects are reduced considerably. It is well known that dynamically generated parton distributions [5] are quite steep in the very small–x region already at rather low Q^2, and in fact steeper [6] than their common 'standard' non–dynamical counterparts. Within this latter standard approach, a full NLO (2–loop) and NNLO (3–loop) analysis morevover confirmed [2, 3] the indications for a perturbative fixed–order instability observed in [1] in the low Q^2 region; even additional resummations have been suggested [7] in order to remedy these instabilities.

It is therefore interesting to study this issue concerning the perturbative stability of $F_L(x,Q^2)$ in the low Q^2 region, $Q^2 \lesssim 5$ GeV^2, within the framework of the dynamical parton model [5, 6]. For this purpose we repeat our previous [8] 'standard' evaluation of the NLO and NNLO distributions within the dynamical approach where the parton distributions at $Q > 1$ GeV are QCD radiatively generated from *valence*–like (positive) input distributions at an optimally determined $Q_0 \equiv \mu < 1$ GeV (where 'valence–like' refers to $a_f > 0$ for *all* input distributions $xf(x,\mu^2) \sim x^{a_f}(1-x)^{b_f}$). This more restrictive ansatz, as compared to the standard approach, implies of course less uncertainties [6] concerning the behavior of the parton distributions in the small–x region at $Q > \mu$ which

is entirely due to QCD dynamics at $x \lesssim 10^{-2}$. The valence–like input distributions at $Q_0 \equiv \mu < 1$ are parametrized according to [8]

$$xq_v(x,Q_0^2) = N_{q_v} x^{a_{q_v}} (1-x)^{b_{q_v}} (1 + c_{q_v}\sqrt{x} + d_{q_v} x + e_{q_v} x^{1.5}) \quad (1)$$

$$xw(x,Q_0^2) = N_w x^{a_w} (1-x)^{b_w} (1 + c_w\sqrt{x} + d_w x) \quad (2)$$

for the valence $q_v = u_v$, d_v and sea $w = \bar{q}$, g densities, and a vanishing strange sea at $Q^2 = Q_0^2$, $s(x,Q_0^2) = \bar{s}(x,Q_0^2) = 0$. All further theoretical details relevant for analyzing F_2 at NLO and NNLO in the $\overline{\rm MS}$ factorization scheme have been presented in [8], using again the QCD-PEGASUS program [9] for the NNLO Q^2–evolutions, appropriately modified to account for the fixed $n_f = 3$ flavor number scheme with a running $\alpha_s(Q^2)$. The heavy flavor (dominantly charm) contribution to F_2 is taken as given by fixed–order NLO perturbation theory [10, 11] using $m_c = 1.3$ GeV and $m_b = 4.2$ GeV as implied by optimal fits [6] to recent deep inelastic c– and b–production HERA data. Since a NNLO calculation of heavy quark production is not yet available, we have again used the same NLO $\mathcal{O}(\alpha_s^2)$ result. This is also common in the literature [12, 13, 14] and the error in the resulting parton distributions due to NNLO corrections to heavy quark production is expected [12] to be less than their experimental errors. Finally, we have used for our fit–analyses the same deep inelastic HERA–H1, BCDMS and NMC data, with the appropriate cuts for $F_2^{p,n}$ as in [8] which amounts to a total of 740 data points. The required overall normalization factors of the data turned out to be 0.98 for H1 and BCDMS, and 1.0 for NMC. We use here again solely deep inelastic scattering data since we are mainly interested in the small–x behavior of structure functions. The resulting parameters of the NLO and NNLO fits are summarized in Table 1. The dynamical gluon and sea distributions, evolved to some specific values of $Q^2 > Q_0^2$, are at the NLO level very similar to the ones in [6] which were obtained from a global analysis including Tevatron Drell–Yan dimuon production and high–E_T inclusive jet data as well. Furthermore, the dynamically generated gluon is steeper as $x \to 0$ than the gluon distributions obtained from conventional 'standard' fits [6, 8](based on some arbitrarily chosen input scale $Q_0 > 1$ GeV^2, i.e. $Q_0^2 \simeq 2$ GeV^2). On

the other hand, the dynamical sea distribution has a rather similar small–x dependence as the 'standard' ones [6, 8]; this is caused by the fact that the valence–like sea input in (2) vanishes very slowly as $x \to 0$ (corresponding to a small value of $a_{\bar{q}}$, $a_{\bar{q}} \simeq 0.07$ according to Table 1) and thus is similarly increasing with decreasing x down to $x \simeq 0.01$ as the sea input obtained by a 'standard' fit. Similar remarks hold when comparing dynamical and standard distributions at NNLO. At NNLO the gluon distribution xg is flatter as x decreases and, in general, falls below the NLO one in the small–x region, typically by 20 – 30% at $x \simeq 10^{-5}$ and $Q^2 \lesssim 10$ GeV^2, whereas the NNLO sea distribution $x\bar{q}$ is about 10 – 20% larger (steeper) than the NLO one. Furthermore it should be mentioned that the NLO $\alpha_s(M_Z^2)$ in Table 1 turns out be somewhat smaller in fits based solely on deep inelastic structure function data [8, 12, 15, 16, 17] as compared to those which take into account additional hard scattering data [2, 6, 18, 19] (for a recent summary, see [20]). At NNLO the resulting $\alpha_s(M_Z^2)$ is generally slightly smaller [20] (c.f. Table 1) which is due to the fact that the higher the perturbative order the faster $\alpha_s(Q^2)$ increases as Q^2 decreases.

Now we turn to the perturbative predictions for $F_L(x, Q^2)$ which can be written as

$$x^{-1}F_L = C_{L,ns} \otimes q_{ns} + \frac{2}{9}\left(C_{L,q} \otimes q_s + C_{L,g} \otimes g\right) + x^{-1}F_L^c \tag{3}$$

where $\otimes$ in the $n_f = 3$ light quark flavor sector denotes the common convolution, q_{ns} stands for the usual flavor non–singlet combination and $q_s = \sum_{q=u,d,s}(q + \bar{q})$ is the corresponding flavor–singlet quark distribution. Again we use the NLO expression [10, 11] for F_L^c also in NNLO due to our ignorance of the $\mathcal{O}(\alpha_s^3)$ NNLO heavy quark corrections. The perturbative expansion of the coefficient functions can be written as

$$C_{L,i}(\alpha_s, x) = \sum_{n=1}\left(\frac{\alpha_s(Q^2)}{4\pi}\right)^n c_{L,i}^{(n)}(x)\,. \tag{4}$$

In LO, $c_{L,ns}^{(1)} = \frac{16}{3}x$, $c_{L,ps}^{(1)} = 0$, $c_{L,g}^{(1)} = 24x(1-x)$ and the singlet–quark coefficient function is decomposed into the non–singlet and a 'pure singlet' contribution, $c_{L,q}^{(n)} = c_{L,ns}^{(n)} + c_{L,ps}^{(n)}$.

Sufficiently accurate simplified expressions for the exact [21, 22] NLO and [23] NNLO coefficient functions $c_{L,i}^{(2)}$ and $c_{L,i}^{(3)}$, respectively, have been given in [1]. It has been futhermore noted in [1] that especially for $C_{L,g}$ both the NLO and NNLO contributions are rather large over almost the entire x–range. Most striking, however, is the behavior of both $C_{L,q}$ and $C_{L,g}$ at very small values [1, 24] of x: the vanishingly small LO parts ($xc_{L,i}^{(1)} \sim x^2$) are negligible as compared to the (negative) constant NLO 2–loop terms, which in turn are completely overwhelmed by the positive NNLO 3-loop singular corrections $xc_{L,i}^{(3)} \sim -\ln x$. This latter singular contribution might be indicative for the perturbative instability at NNLO [1], as discussed at the beginning, but it should be kept in mind that a small–x information alone is *insufficient* for reliable estimates of the convolutions occurring in (3) when evaluating physical observables.

For this latter reason we do not display the individual gluon and (sea)quark distributions separately but instead our predictions for the convolutions of the individual light u, d, s quark (F_L^q) and gluon (F_L^g) contributions in (3) in Figs. 1 and 2, respectively, at two characteristic low values of Q^2. (Note that $F_L^q + F_L^g = F_L - F_L^c$ according to (3)). Although the perturbative instability of the subdominant quark contribution in Fig. 1 as obtained in a 'standard' fit does not improve dramatically for the dynamical (sea) quark distributions, the instability disappears almost entirely for the dominant dynamical gluon contribution already at $Q^2 \simeq 2$ GeV^2 as shown in Fig. 2. This implies that the dynamical predictions for the total $F_L(x, Q^2)$ become perturbatively stable already at the relevant low values of $Q^2 \gtrsim \mathcal{O}(2 - 3$ GeV$^2)$ as evident from Fig. 3, in contrast to the 'standard' results in Fig. 4. In the latter case the stability has not been fully reached even at $Q^2 = 5$ GeV^2 where the NNLO result at $x = 10^{-5}$ is more than 20% larger than the NLO one. A similar discrepancy prevails for the dynamical predictions in Fig. 3 at $Q^2 = 2$ GeV^2. This is, however, not too surprising since $Q^2 = 2$ GeV^2 represents somehow a borderline value for the leading twist–2 contribution to become dominant at small x values. This is further corroborated by the observation that the dynamical NLO twist–2 fit slightly

undershoots the HERA data for F_2 at $Q^2 \simeq 2$ GeV^2 in the small–x region (cf. Fig. 1 of [6]). The NLO/NNLO instabilities implied by the standard fit results obtained in [2, 3] at $Q^2 \lesssim 5$ GeV^2 are even more violent than the ones shown in Fig. 4. This is mainly due to the negative longitudinal cross section (negative $F_L(x, Q^2)$) encountered in [2, 3]. The perturbative stability in any scenario becomes in general better the larger Q^2, typically beyond 5 GeV^2 [1, 2, 3], as shown in Figs. 3 and 4. This is due to the fact that the Q^2–evolutions eventually force any parton distribution to become sufficiently steep in x.

For completeness we finally compare in Fig. 5 our dynamical (leading twist) NNLO and NLO predictions for $F_L(x, Q^2)$ with a representative selection of (partly preliminary) HERA–H1 data [25, 26]. Our results for F_L, being gluon dominated in the small–x region, are in full agreement with present measurements which is in contrast to expectations [2, 3] based on negative parton distributions and structure functions at small values of x. To illustrate the manifest positive definiteness of our dynamically generated structure functions at $Q^2 \geq \mu^2 = 0.5$ GeV^2 we show $F_L(x, Q^2)$ in Fig. 5 down to small values of Q^2 although leading twist–2 predictions need not necessarily be confronted with data below, say, 2 GeV^2.

To summarize, we have shown that the extreme perturbative NNLO/NLO instability of the longitudinal structure function F_L at low Q^2, noted in [2–4], is an artifact of the commonly utilized 'standard' gluon distributions rather than an indication of a genuine problem of perturbative QCD. In fact we have demonstrated that these extreme instabilities are reduced considerably already at $Q^2 = 2 - 3$ GeV^2 when utilizing the appropriate, dynamically generated, parton distributions at NLO and NNLO. These latter parton distributions have been obtained from a NLO and NNLO analysis of $F_2^{p,n}$ data, employing the concepts of the dynamical parton model. It is gratifying to notice, once again, the advantage of the dynamical parton model approach to perturbative QCD.

References

[1] S. Moch, J.A.M. Vermaseren, A. Vogt, *Phys. Lett.* **B606** (2005) 123, and references therein

[2] A.D. Martin et al., *Phys. Lett.* **B531** (2002) 216

[3] A.D. Martin, W.J. Stirling, R.S. Thorne, *Phys. Lett.* **B635** (2006) 305

[4] R.S. Thorne, Proceedings of the Ringberg Workshop on 'New Trends in HERA Physics' (Tegernsee, Oct. 2005), p. 359 (hep–ph/0511351)

[5] M. Glück, E. Reya, A. Vogt, *Eur. Phys. J.* **C5** (1998) 461

[6] M. Glück, P. Jimenez–Delgado, E. Reya, DO–TH 07/06 (arXiv:0709.0614v2), to appear in Eur. Phys. J. **C**

[7] C.D. White, R.S. Thorne, *Phys. Rev.* **D75** (2007) 034005

[8] M. Glück, C. Pisano, E. Reya, *Eur. Phys. J.* **C50** (2007) 29

[9] A. Vogt, *Comput. Phys. Commun.* **170** (2005) 65

[10] E. Laenen et al., *Nucl. Phys.* **B392** (1993) 162

[11] S. Riemersma, J. Smith, W.L. van Neerven, *Phys. Lett.* **B347** (1995) 143

[12] S.I. Alekhin, *Phys. Rev.* **D68** (2003) 014002

[13] S.I. Alekhin, *JETP Lett.* **82** (2005) 628

[14] S.I. Alekhin, K. Melnikov, F. Petriello, *Phys. Rev.* **D74** (2006) 054033

[15] A.L. Kataev et al., *Phys. Lett.* **B388** (1996) 179; **B417** (1998) 374

[16] M. Glück, E. Reya, C. Schuck, *Nucl. Phys.* **B754** (2006) 178

[17] J. Blümlein, H. Böttcher, A. Guffanti, *Nucl. Phys.* **B** (Proc. Suppl.) **135** (2004) 152; *Nucl. Phys.* **B774** (2007) 182

[18] J. Pumplin et al., CTEQ Collab., *JHEP* **07** (2002) 012

[19] W.K. Tung et al., CTEQ Collab., *JHEP* **02** (2007) 053

[20] J. Blümlein, DIS 2007 (Munich, April 2007), arXiv:0706.2430

[21] J. Sanchez Guillen et al., *Nucl. Phys.* **B353** (1991) 337

[22] E.B. Zijlstra, W.L. van Neerven, *Phys. Lett.* **B273** (1991) 476

[23] J.A.M. Vermaseren, A. Vogt, S. Moch, *Nucl. Phys.* **B724** (2005) 3

[24] S. Catani, F. Hautmann, *Nucl. Phys.* **B427** (1994) 475

[25] C. Adloff et al., H1 Collab., *Eur. Phys. J.* **C21** (2001) 33; **C30** (2003) 1

[26] E.M. Lobodzinska, H1 Collab., DIS 2004 (Strbske Pleso, Slovakia), hep–ph/0311180; T. Lastovicka, H1 Collab., *Eur. Phys. J.* **C33** (2004) s388

Table 1: Parameter values of the NNLO and NLO QCD fits with the parameters of the input distributions referring to (1) and (2) at a common input scale $Q_0^2 = \mu^2 = 0.5$ GeV^2 which turns out to be optimal at both perturbative orders.

	NNLO				NLO			
	u_v	d_v	$\bar{q}$	g	u_v	d_v	$\bar{q}$	g
N	0.6092	0.2187	0.1055	22.875	0.5118	0.286845	0.1778	47.080
a	0.3239	0.8603	0.0705	0.9707	0.3096	0.8513	0.0670	1.3195
b	2.7135	4.7369	10.273	6.7931	2.8053	4.6510	13.982	10.443
c	-9.2103	60.908	10.329	—	-8.5243	45.559	-0.9923	2.8940
d	53.545	1.6192	-8.1010	—	54.966	-5.3465	21.108	—
e	-41.119	-36.977	—	—	-40.095	-21.832	—	—
χ^2/dof	1.067				1.069			
$\alpha_s(M_Z^2)$	0.112				0.113			

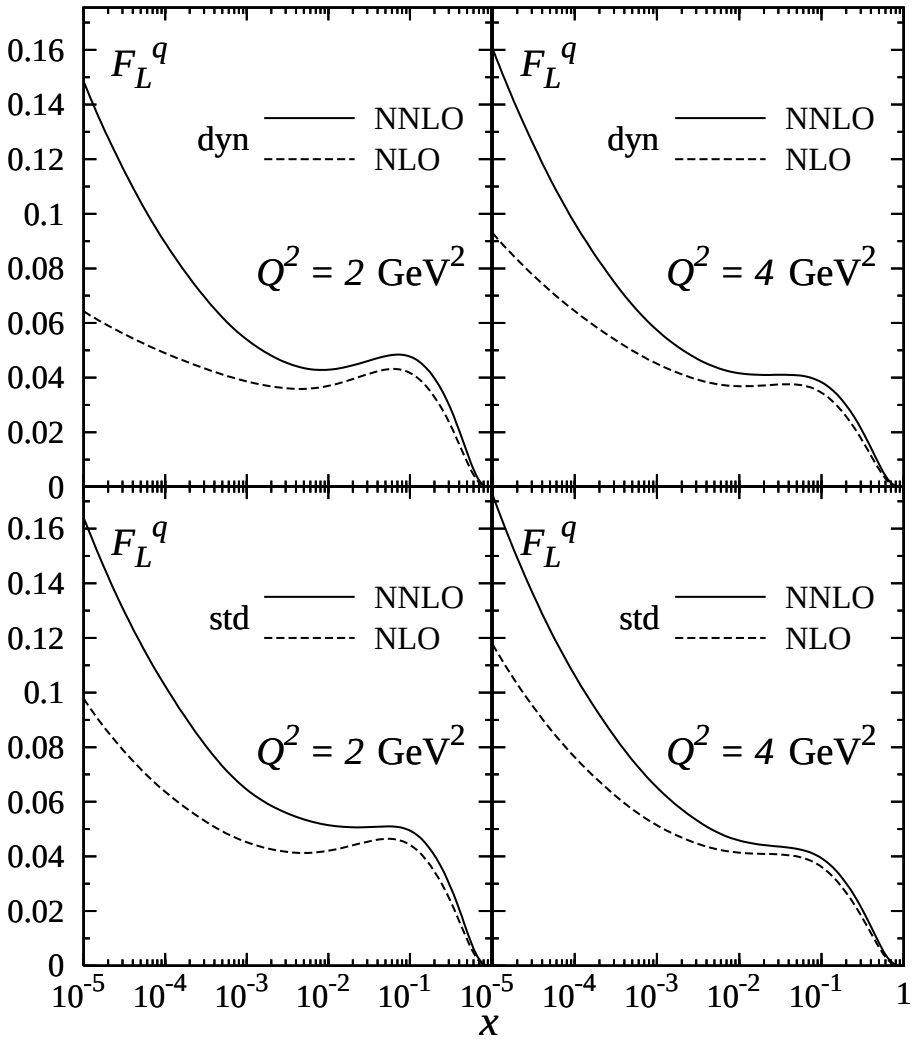


Figure 1: The individual light (u, d, s) quark contribution F_L^q to the total F_L in (3) in the dynamical (dyn) and standard (std) parton approach at NNLO and NLO for two representative low values of Q^2. The standard parton distributions utilized in the lower panel are taken from [8]. Our standard NLO results in the lower panel are similar for the CTEQ6 (anti)quark distributions [18]. Notice that, according to (3), $F_L^q + F_L^g = F_L - F_L^c$.

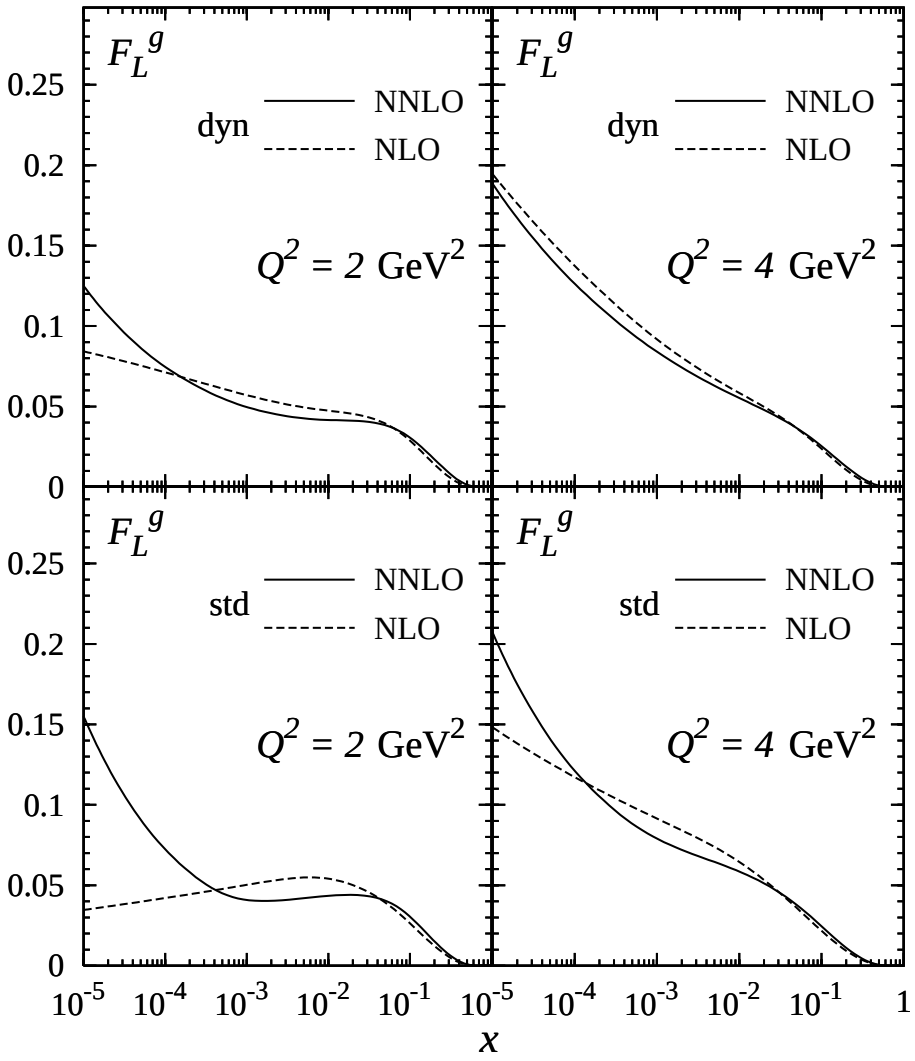


Figure 2: As in Fig. 1 but for the gluonic contribution F_L^g to F_L in (3) with $F_L^g = \frac{2}{9} x\, C_{L,g} \otimes g$.

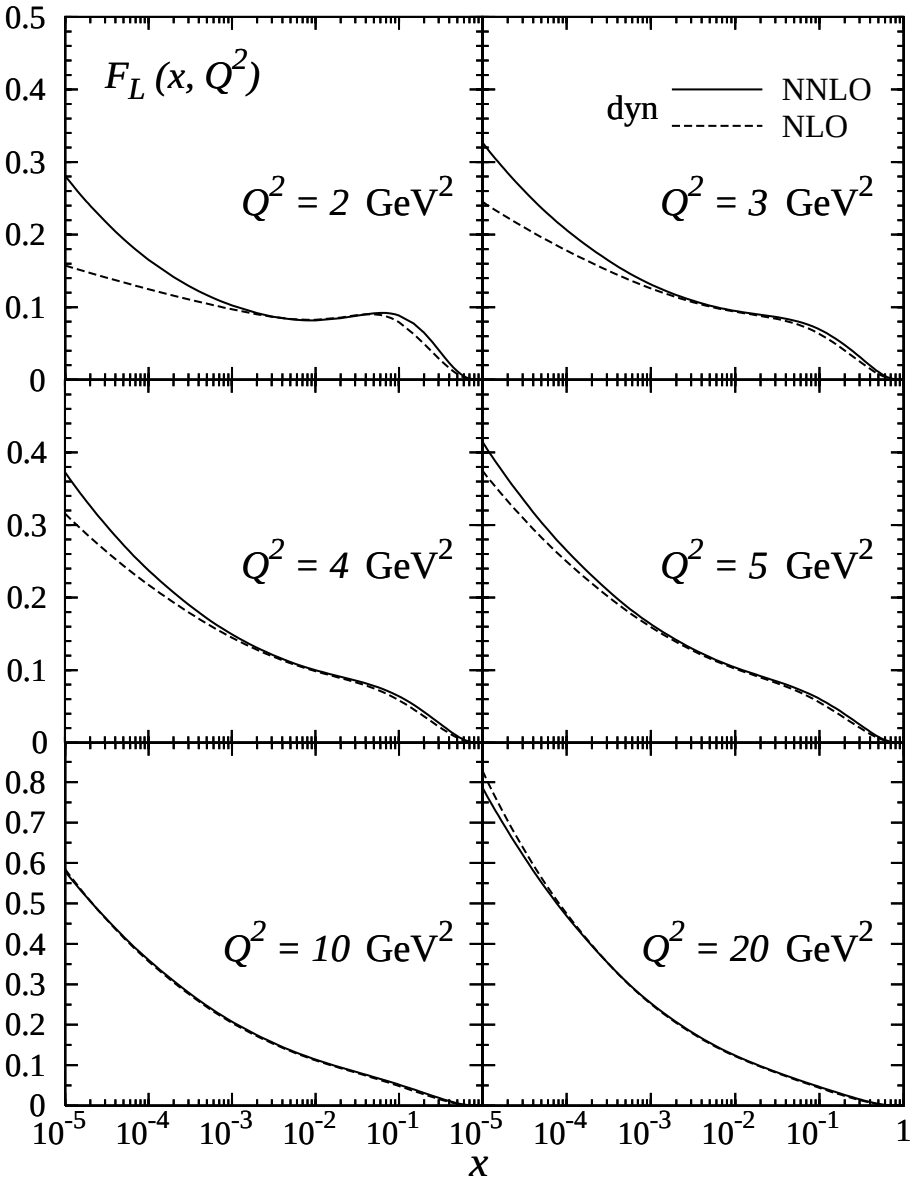


Figure 3: Dynamical parton model NNLO and NLO predictions for $F_L(x, Q^2)$ in (3).

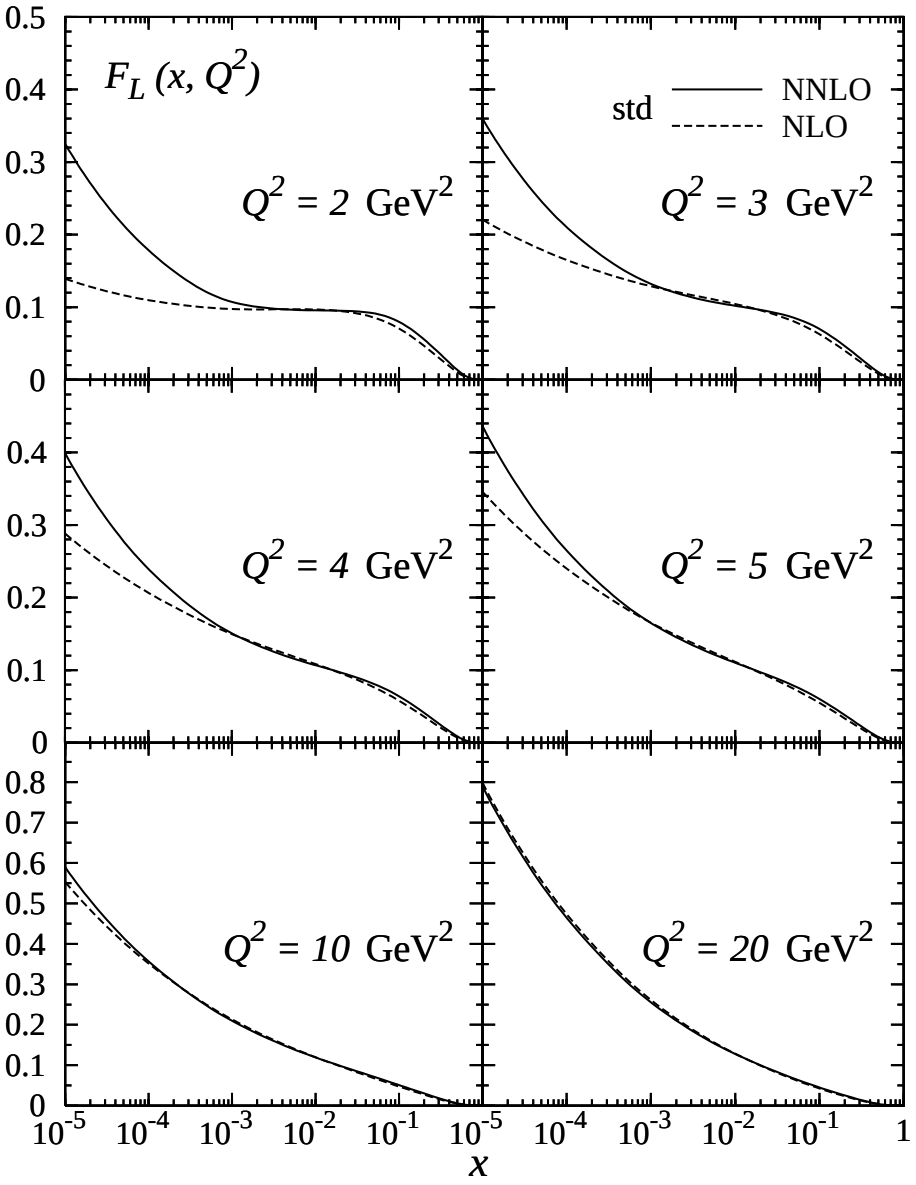


Figure 4: As in Fig. 3 but for the common standard parton distributions as taken, for example, from [8].

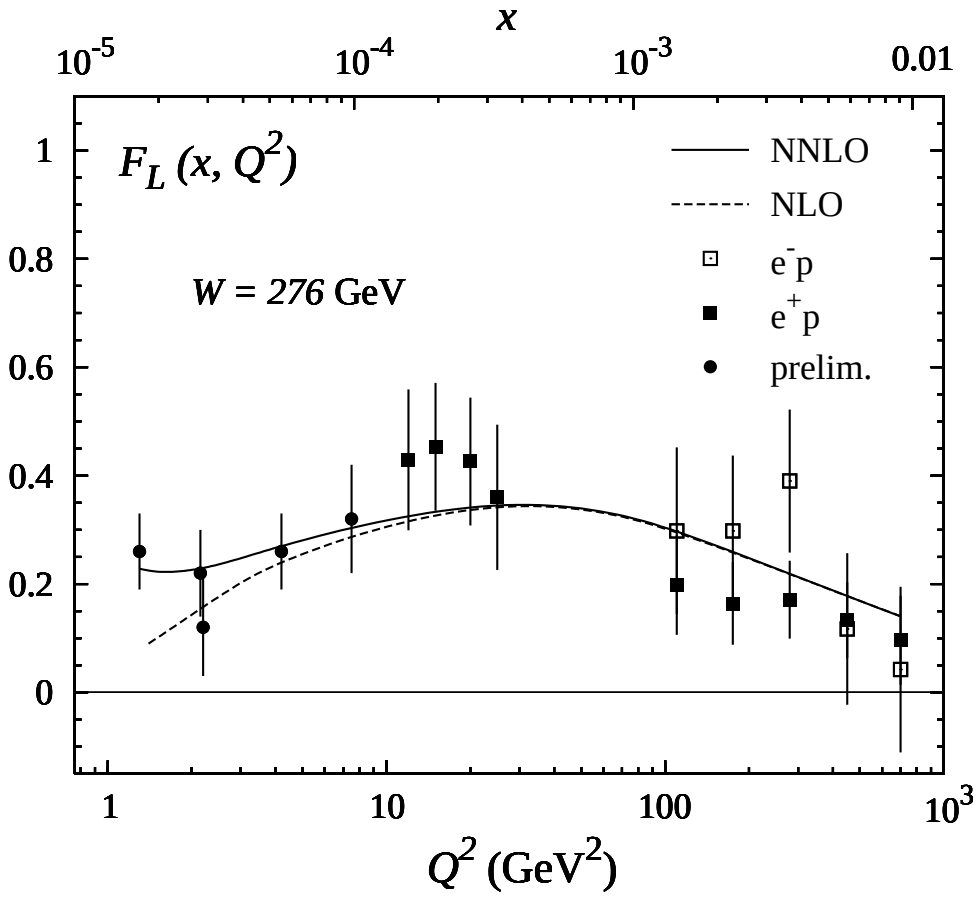


Figure 5: Our dynamical NNLO and NLO predictions for F_L at a fixed value of $W = 276$ GeV. The (partly preliminary) H1 data [25, 26] are at fixed $W \simeq 276$ GeV.